Arabian Journal of Chemistry (2022) **15**, 103820

King Saud University

Arabian Journal of Chemistry

www.ksu.edu.sa
www.sciencedirect.com

ORIGINAL ARTICLE

Cysteine combined with carbon black as support for electrodeposition of poly (1,8-Diaminonaphthalene): Application as sensing material for efficient determination of nitrite ions

Ouissal Salhi, Tarik Ez-zine, Larbi Oularbi, Mama El Rhazi *

University Hassan II Casablanca, Faculty of Sciences and Technologies, Laboratory of Materials Membranes and Environment, P.B 146, Mohammedia 20800, Morocco

Received 12 January 2022; accepted 24 February 2022
Available online 2 March 2022

KEYWORDS

Nitrite detection;
1,8-Diaminonapthalene;
Cysteine;
Carbon black;
Nanohybrid material;
Electrochemical sensor

Abstract Poly 1,8-Diaminonaphtahlene/cysteine (poly 1,8-DAN/Cys) combined with carbon black (CB) nanoparticles are proposed as an excellent sensor for the detection of nitrite ions. To design the electrocatalyst, a simple approach consisting on drop-casting method was applied to disperse carbon black on the surface of glassy carbon electrode, followed by the immobilization of cysteine on the surface of CB nanoparticles. The electrochemical polymerization of 1,8-Diaminonaphthalene was conducted in acidic medium by using cyclic voltammetry. The prepared hybrid material was denoted poly 1,8-DAN /Cys/CB. Several methods were used to characterize the structural and electrochemical behavior of the reported hybrid material including Fourier transform infrared spectroscopy (FTIR), Scanning electron microscopy (SEM), cyclic voltammetry (CV), electrochemical impedance spectroscopy (EIS), amperometry and differential pulse voltammetry (DPV). The prepared electrode displayed an outstanding electroactivity towards nitrite ions reflected by an enhancement in the intensity of the current and a decrease of the charge transfer resistance. Poly 1,8-DAN/Cys/CB displayed an excellent sensing performance towards the detection of nitrite with a very low detection limit of 0.25 μM. Two linear ranges of 1–40 μM and 20–210 μM when using amperometry and differential pulse voltammetry (DPV) were obtained respectively. This work highlights the simple preparation of a polymeric film rich in amine and thiol groups for nitrite detection.

© 2022 The Authors. Published by Elsevier B.V. on behalf of King Saud University. This is an open access article under the CC BY-NC-ND license (http://creativecommons.org/licenses/by-nc-nd/4.0/).

* Corresponding author.
E-mail address: elrhazim@hotmail.com (M. El Rhazi).
Peer review under responsibility of King Saud University.

Production and hosting by Elsevier

1. Introduction

The over-consumption of nitrite leads to several health defects such as cancer, methemoglobinemia, and Baby Blue syndrome (Annalakshmi et al., 2020). It was reported that some amine in the human stomach can react with nitrites and nitrates to form carcinogenic nitrosamines

https://doi.org/10.1016/j.arabjc.2022.103820
1878-5352 © 2022 The Authors. Published by Elsevier B.V. on behalf of King Saud University.
This is an open access article under the CC BY-NC-ND license (http://creativecommons.org/licenses/by-nc-nd/4.0/).

(Buller et al., 2021). It can also react with the hemoglobin in the blood system to form methemoglobin which cannot transport the oxygen to the organisms (Mudan et al., 2020). In this context, the World Health Organization (WHO) has added nitrite on the list of the hazardous pollutant (Annalakshmi et al., 2020). The concentration of 3 mg/L (65.2 μM) was defined as maximum allowable concentration admissible in drinking water (Organization, 2011). Unfortunately, nitrite is still being used in industrial processes as food preservative and soil fertilizer (Cvetković et al., 2019; Wu et al., 2021). In view of this, numerous methods have been developed for monitoring nitrite ions (Wang et al., 2017; Mahmud et al., 2020; Mako et al., 2020). Among them, electrochemical techniques are more suitable for many different application needs owing to their rapidity, sensitivity, low cost, and portability (Zanfrognini et al., 2020; El Rhazi et al., 2018; Oularbi et al., 2020; Oularbi et al., 2019; Salih et al., 2017; Oularbi, 2018). These methods are based on the use of modified electrodes with suitable materials which offer a very high surface area, and a good electronic transfer (Deroco et al., 2018). Among carbon nanomaterials, Carbon black (CB) constitutes an amorphous and low-cost material (the cost does not exceed 1 €/Kg) (Deroco et al., 2018). In fact, it is produced by partial combustion of industrial organic matter to small particles with a diameter in the range of nm (Mazzaracchio et al., 2019). CB exhibits excellent electrical properties and allows facile and rapid modification of the electrodes (by drop-casting), which makes CB suitable to develop cost-effective electrochemical devices (Baccarin et al., 2017; Ibáñez-Redín et al., 2018). Poly diaminonaphthalene derivates (PDAN) are semiconducting polymers composed from the repetition of naphthalene rings containing primary (—N═C), secondary amine (—NH—C), and free amine (—NH_2) functional groups (Bhatt et al., 2021). The presence of aminated structure makes PDAN an excellent choice to develop substrates for the electrodeposition of different metallic nanoparticles as mentioned in many papers (Chemchoub et al., 2020; Halim et al., 2021; Shi et al., 2019; Chemchoub et al., 2019).

Several hybrid materials based on conducing polymers such as polyaniline (PANI), polypyrrole (PPy), and polyethylenedioxythiophene (PEDOT), have been reported for the electrochemical sensing of nitrite ions and many other applications (Xiao et al., 2018; Chen and Zheng, 2021; Ge et al., 2020; Salhi et al., 2021; El Attar et al., 2022; El Attar et al., 2020; El Attar et al., 2021). However, their preparation requires chemical polymerization which is time consuming and involves the use of numerous chemical reagents, or they are usually combined with expensive metals such as silver, gold, and palladium (Shi et al., 2019; Kaladevi et al., 2020; Ma et al., 2014).

Herein, a very simple and quick strategy was adopted to develop a low-cost material based on carbon black, cysteine, and poly (1,8-Diaminonaphtalene). Briefly, the surface of the electrode (GCE) was modified with CB suspension and cysteine solution (Cys), followed by the electropolymerization of the monomer 1,8-Diaminonaphthalene in acidic medium. The structural and electrochemical behavior as well as the application of the reported sensor for nitrite detection were investigated and optimized. To the best of our knowledge, no similar studies have been devoted to the combination of polymer and Cysteine / CB as sensing material for nitrite detection.

2. Experimental

2.1. Apparatus

The structural properties of the obtained materials were examined using Fourier transform infrared spectroscopy (FTIR) with an Affinity-1S SHIMADZU spectrometer. The morphological properties of CB, Cys/CB, and poly 1,8-DAN/Cys/CB were characterized using scanning electron microscopy (FEI FEG 450) coupled to EDX spectrum (BURKER XFlash 6/30). The electrochemical measurements were carried out using a VersaSTAT 4 potentiostat/galvanostat controlled with VersaStudio software. A standard electrochemical cell with three electrodes: the modified glassy carbon electrode (GCE) as the working electrode, a silver/silver chloride electrode (Ag/AgCl) as the reference electrode, and a platinum electrode as the counter electrode was used.

2.2. Reagents

Graphite powder, paraffin oil, 1,8-diaminonaphthalene (1,8-DAN), potassium Ferri- Ferrocyanide ($K_3Fe(CN)_6/K_4Fe(CN)_6{\cdot}3H_2O$; ACS reagent > 99%), disodium hydrogen phosphate ($Na_2HPO_4{\cdot}7H_2O$), sodium dihydrogen phosphate dihydrate ($NaH_2PO_4{\cdot}2H_2O$), and cysteine hydrochloride were purchased from Sigma Aldrich. Carbon black powder (CB) N220 was obtained from Cabot Corporation. Hydrochloric acid (HCl, 37%) was acquired from Labo Chimie. Sodium nitrite ($NaNO_2$, ACS reagent > 98%) was procured from Panreac Quimica. Bi-distillated water was used to prepare all the analytical solutions.

2.3. Elaboration of modified electrodes

Alumina with different size particles (1, 0.3, and 0.05 μm) were used to polish the surface of GCE. Then it was sonicated for 3 min in a solution of ethanol: water (1:1) before to be treated with 0.1 M solution of HCl. The modification of the electrodes was performed as follow. Firstly, 6 μL of carbon black (CB) suspension of concentration 1 mg/ml was drop casted on the electrode surfaces. The CB/GCE electrodes were afterwards placed in a solution of 1 mM of cysteine (Cys) for 3 min. The electrochemical deposition of 1,8-Diaminonaphthalene was carried out by using cyclic voltammetry in a potential range between −0.2 to 1 V *vs.* Ag/AgCl at a scan rate of 50 mV/s in a solution containing 5 mM of the monomer in 0.1 M HCl.

3. Results and discussion

3.1. Electropolymerization of 1,8-Diaminonaphthalene

The polymerization of 1,8-Diaminonaphthalene was carried out using the most used electrochemical techniques which is cyclic voltammetry in a solution containing 5 mM of the monomer in the potential range between −0.2 to 1.0 V *vs.* Ag/AgCl for 10 cycles at the scan rate of 50 mV/s. For the purpose of comparison, the 1,8-Diaminonaphthalene was electropolymerized on the three electrodes: bare GCE, CB/GCE and Cys/CB/GCE. The corresponding voltammograms are displayed in Fig. 1a, Fig. 1b and Fig. 1c. The electrochemical synthesis of poly 1,8-Diaminonaphthalene was limited to ten cycles for this study. On all the electrodes, an irreversible oxidation peak was observed during the first cycle which is attributed to the electrooxidation of the monomer leading to the radical cation as reported earlier in the literature (Majid et al., 2003). However, we can note that on CB/GCE (red line), the first anodic oxidation potential appears at 0.44 V *vs.* Ag/AgCl whereas this value was 0.51 V on GCE, and the current intensity increased by 17.2% compared to GCE. This

behavior can be explained by the large surface area provided by CB nanoparticles (Hwa et al., 2019). This behavior is even accentuated after the immobilization of cysteine onto the surface of CB/GCE providing an oxidation potential of 0.41 V with a further increase of the current intensity. It should be mentioned that the intensity of the first peak for all the electrodes was decreased gradually and the oxidation peak of 1,8-Diaminonaphthalene disappeared completely while a small oxidation/reduction peaks appeared at E_{pa} = 0.22 V and E_{pc} = 0.1 V and were increased gradually for the subsequent cycles indicating the formation of the electroactive poly 1,8-Diaminonaphthalene film as described earlier by many authors (Majid et al., 2003; Oyama et al., 1989; Tagowska et al., 2005). However, we can note that a well-defined peaks with a higher current were observed with Cys/CB/GCE.

Based on all the above results, we can suggest two possible hypotheses: i) the nature of the substrate has a significant impact on the electropolymerizaton of 1,8-Diaminonaphthalene, ii) the combination of cysteine and CB nanoparticles promotes the formation of poly 1,8-Diaminonaphthalene film. This can be explained by a possible interaction between the functional groups of cysteine and 1,8-Diaminonaphthalene. In fact, cysteine is an amino acid with an isoelectric point of 5.06 which means that the adsorbed layer of cysteine can be charged either positively or negatively depending on the pH of adjacent solution. The charge of the surface is an important parameter as reported by sanders et al., (Sanders and Anderson, 2009). We can therefore ensure an excess of charge by playing on the pH of the solution which enhances the electrostatic deposition of radical cations of 1,8-diaminonaphthalene onto cysteine monolayers during the electropolymerization. It should be noted that the same behavior was observed when the polymerization of 1,8-Diaminonaphthalene was conducted on carbon nanotubes (Nguyen et al., 2011). Noting that poly 1,8-Diaminonaphthalene is oxidized in acidic medium at positive potential to produce cationic radials which react together to promote the polymerization (Lee et al., 1992).

3.2. Morphological and structural characterizations

The morphology of the modified electrodes was investigated by Scanning Electron Microscopy (SEM) coupled to an EDX detector. The SEM images of CB, Cys/CB, and poly 1,8-DAN/Cys/CB are illustrated in Fig. 2.a. The surface of CB was uniform with small nanoparticles which indicates that CB is well dispersed at the electrode surface as reported by Cinti et al., (Cinti et al., 2015). The surface of Cys/CB illustrated in was rougher and has more fibrous-like shape (Kingsford et al., 2019). While after the electrodeposition of poly 1,8-Diaminonaphthalene, the surface of the electrode showed a homogeneous dispersion of spherical nanoparticles. The same results were observed by Nguyen et al., when the 1,8-Diaminonaphthalene was electropolymerized on carbon nanotubes (Nguyen et al., 2011).

In order to verify the presence of thiol and amine groups on the surface of the working electrode, the elemental mapping of poly 1,8-DAN/Cys/CB was performed. The corresponding results displayed in Fig. 2.b confirm the presence of carbon, sulfur, and azote which proves the successful formation of poly 1,8-DAN/Cys/CB.

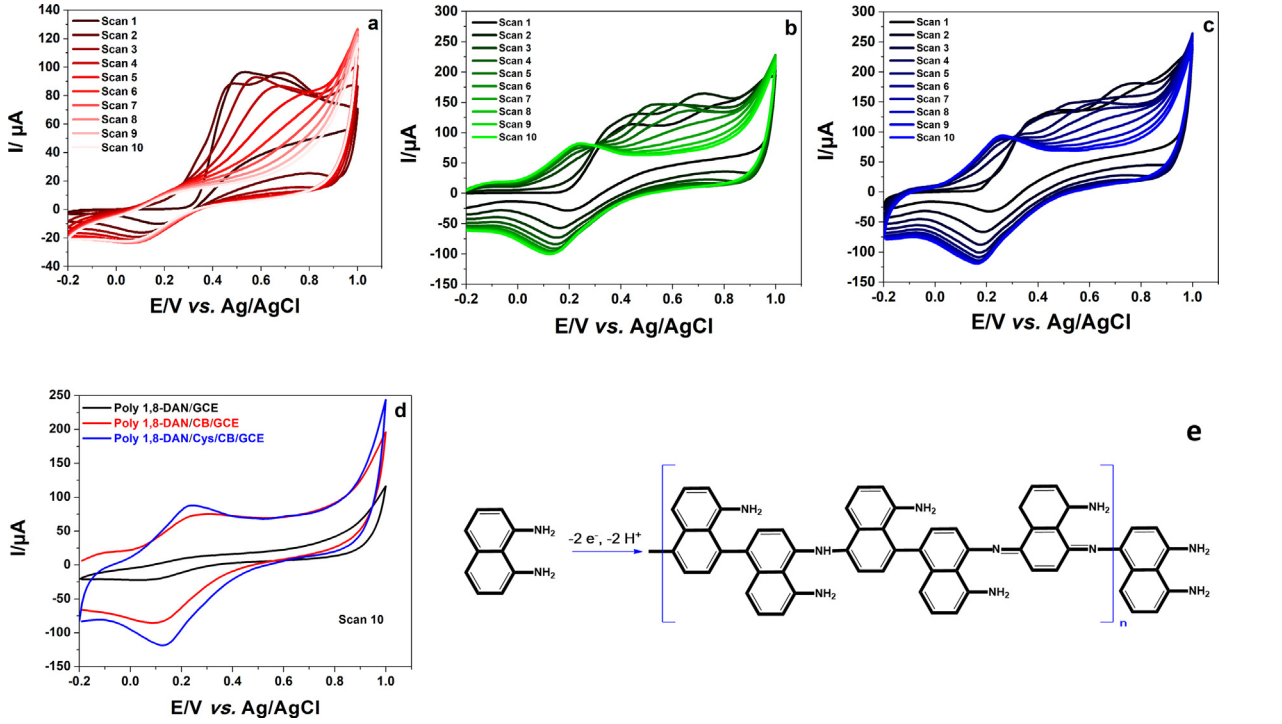

Fig. 1 Electrochemical polymerization of 1,8-Diaminonaphthalene on **a)** GCE, **b)** CB/GCE, **c)** Cys/CB/GCE. **d)** The scan 10 on GCE (black line), CB/GCE (red line), and Cys/CB/GCE (blue line). **e)** Electropolymerization mechanism of 1,8-Diaminonaphthalene (Lee et al., 1992).

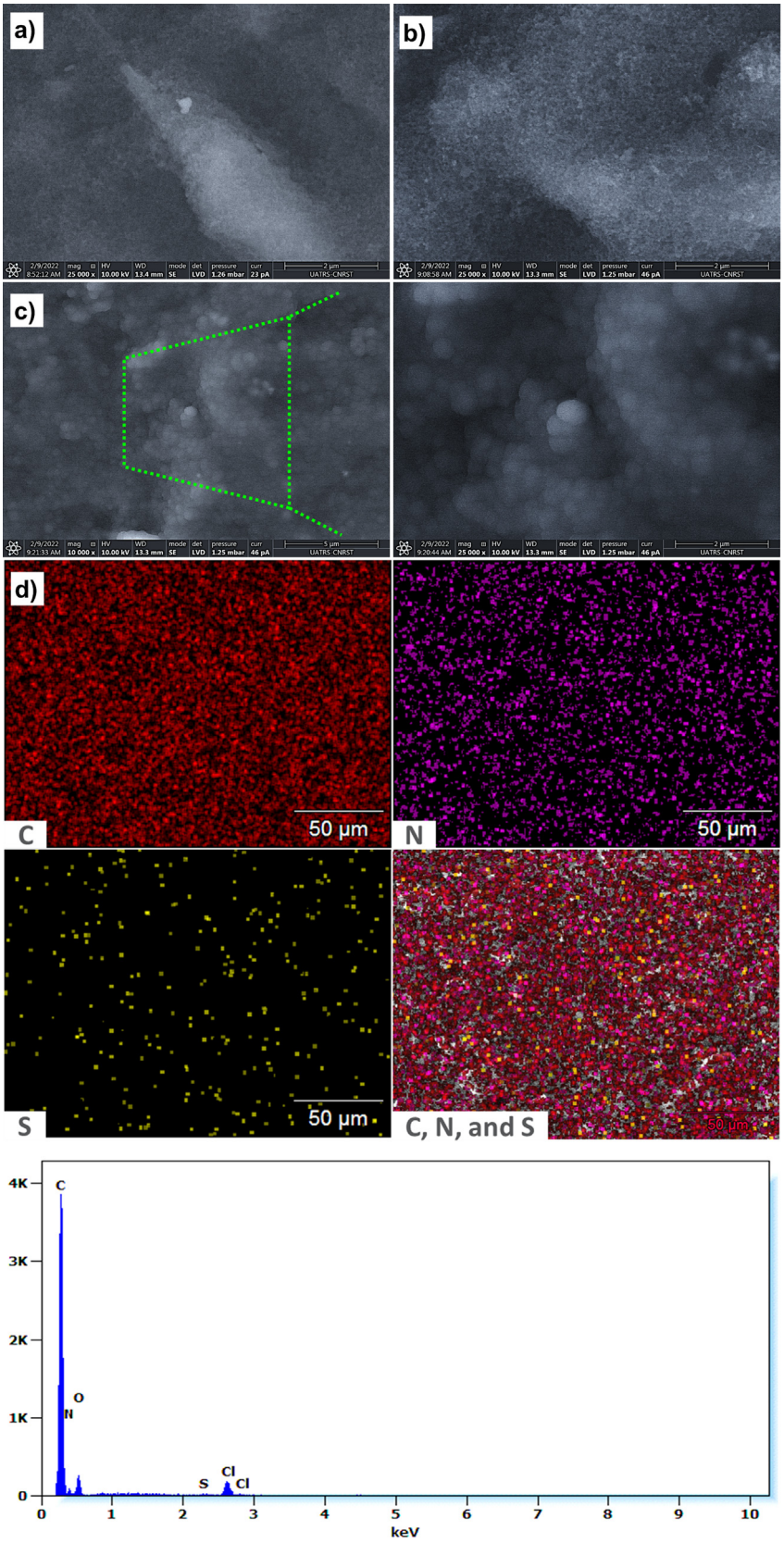

Fig. 2 SEM images of **a)** CB, **b)** Cys/CB, and **c)** poly 1,8-DAN/Cys/CB. **d)** Elemental mapping and EDS of poly 1,8-DAN/Cys/CB. **e)** FTIR spectra of CB (black line), Cys/CB (red line), poly 1,8-DAN/Cys/CB (blue line).

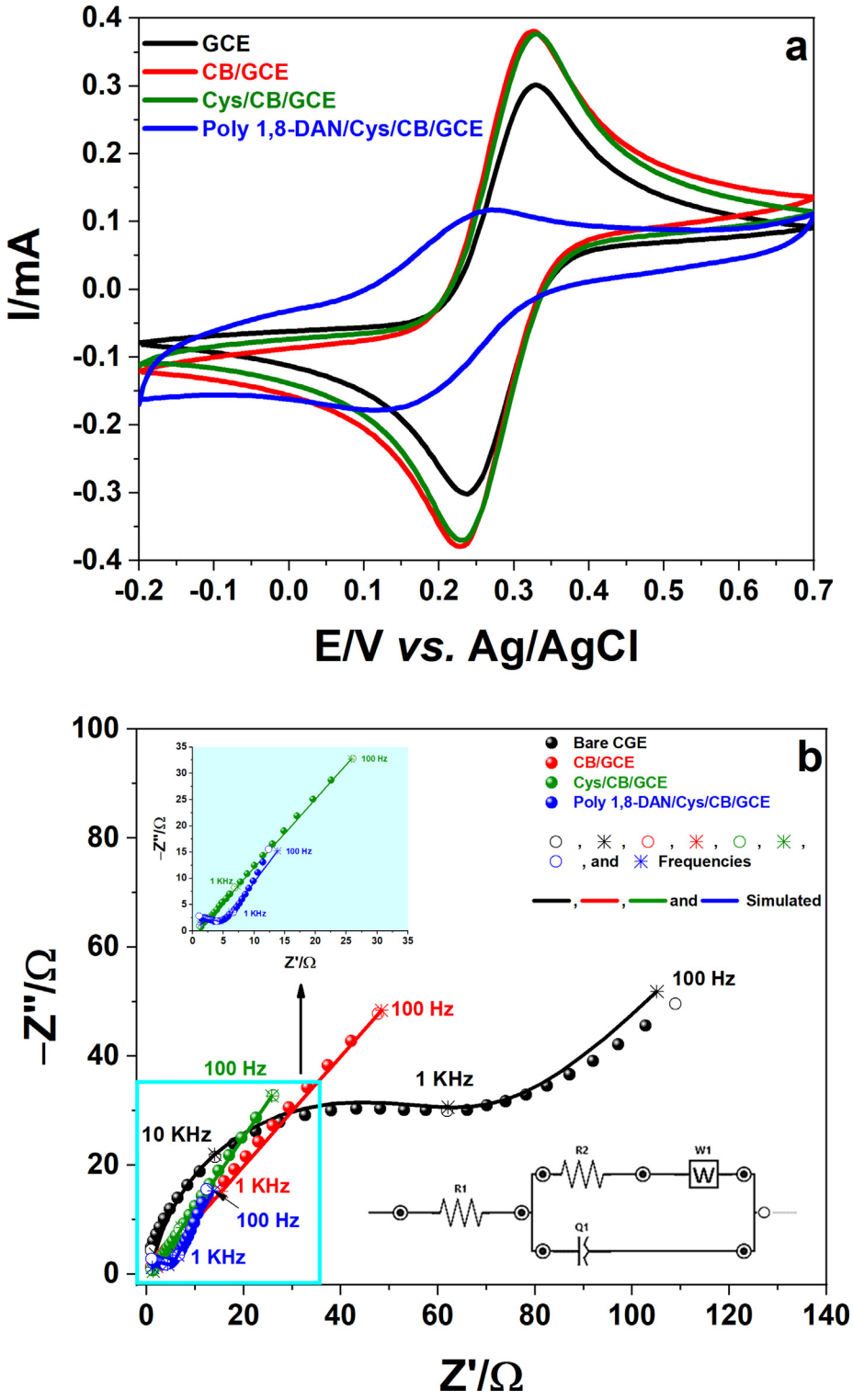

Fig. 3 **a)** Cyclic voltammetry of GCE (black line), CB/GCE (red line), and poly 1,8-DAN/Cys/CB/GCE (blue line). **b)** Nyquist Plots of GCE (black), CB/GCE (red), Cys/CB/GCE (green), and poly 1,8-DAN/Cys/CB/GCE (blue) in 0.5 M of KCl containing 10 mM of [Fe(CN]6]3-/4- at a fixed potential of 0.35 V *vs.* Ag/AgCl and an amplitude of 10 mV.

The chemical structure of CB, Cys/CB, and poly 1,8-DAN/Cys/CB were also examined using FTIR spectroscopy, and the obtained spectrums are displayed in Fig. 2. The FTIR of CB (black line) showed an absorption peak at 1646 cm^{-1} which is ascribed to C═C vibration. Two others bands were observed at 967 and 3640 cm^{-1} indicating the presence of C—O and O—H groups (He et al., 2015; Xie et al., 2019). In the spectrum of Cys/CB (red line), new bands were observed. In fact, the band at 1113, 1169, and 1695 cm^{-1} can be attributed to amine group of cysteine (Dokken et al.,

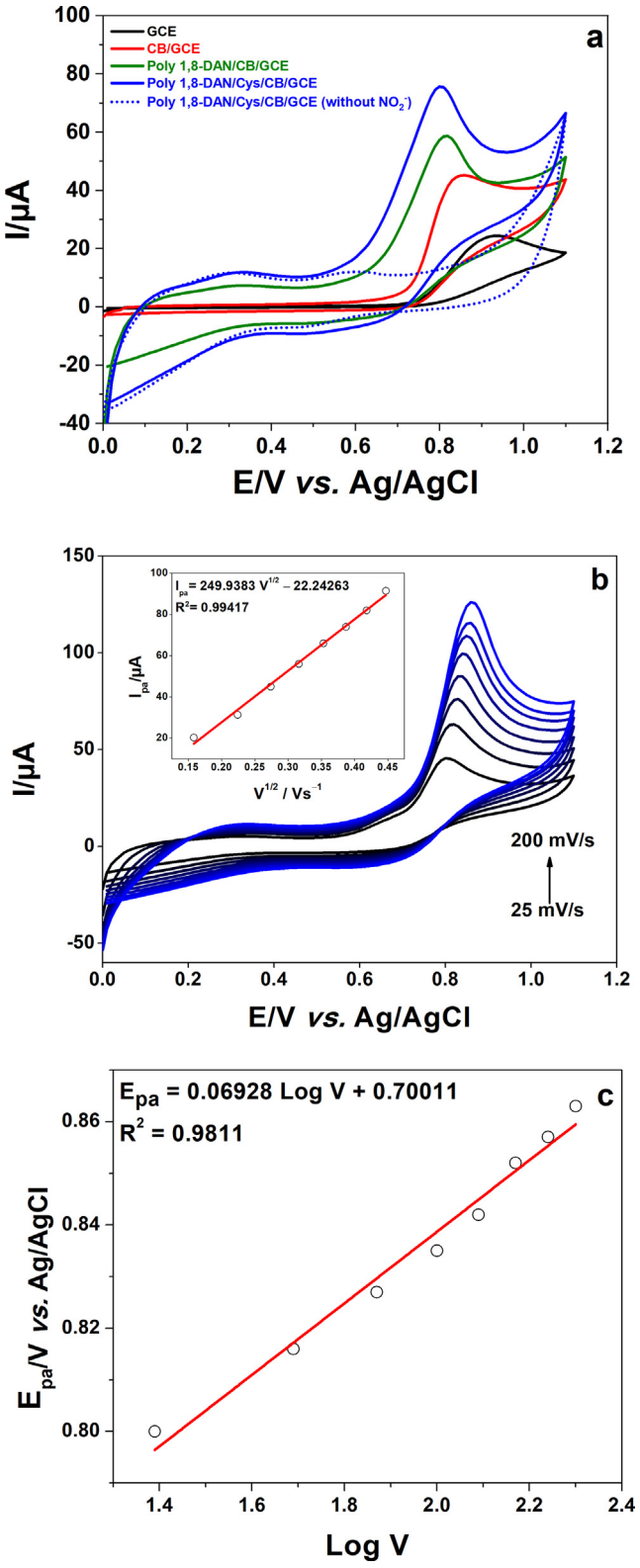

Fig. 4 **a)** Cyclic voltammetry of GCE (black line), CB/GCE (red line), poly 1,8-DAN/CB/GCE (green line), and poly 1,8-DAN/Cys/CB/GCE (blue line) in pH 7.2, 0.1 M PBS with 1 mM of NO_2^- at a scan rate of 50 mV/s, and without NO_2^- (dashed line). **b)** Cyclic voltammetry of poly 1,8-DAN/Cys/CB/GCE in pH 7.2, 0.1 M PBS containing 1 mM of NO_2^- at scan rates from 25 to 200 mV/s with the plot of NO_2^- oxidation peak current versus $V^{1/2}$. **c)** The calibration curve of the oxidation peak potential versus log V.

2009). In addition to this, new bands were noticed at 532, 653, and 717 cm^{-1} revealing the presence of thiol and carboxylic acid groups of cysteine as reported earlier by Parsons et al., (Parsons et al., 2013). The structural properties of poly 1,8-DAN/Cys/CB were also illustrated (blue line). The presence of the bands located at 1488 and 1593 cm^{-1} indicates the presence of C=C of the aromatic rings, while, the absorption peaks in 1224 and 1312 cm^{-1} are attributed to C—N stretching. Two other absorption bands were observed at 3480 cm^{-1} and 1663 cm^{-1} corresponding to N—H and NH_2 vibrations (Nasalska and Skompska, 2003). Our Finding confirm the successful polymerization of poly 1,8-DAN as suggested previously by many authors (Nasalska and Skompska, 2003; Pałys et al., 1997), and also the presence of thiol groups.

3.3. Electrochemical characterizations of modified electrodes

The electrochemical behavior of the prepared electrodes were investigated by Cyclic voltammetry (CV) in a solution containing 10 mM $[Fe(CN)_6]^{3-/4-}$, 0.5 M KCl at 100 mV/s. The corresponding graphs are displayed in Fig. 3a. We can notice that an important increase of the current intensities after the addition of CB on the surface of GCE (red line). The current is about 402 µA with a separation of peak-to peak around 93 mV, while the current on GCE (black line) is about 317 µA. This enhancement can be explained by the excellent electrical properties and high surface area of carbon black nanoparticles as mentioned earlier by many authors (Mazzaracchio et al., 2019; Arduini et al., 2020). After the immobilization of cysteine on the surface of CB/GCE (green line), the same behavior as on CB/GCE was observed in the presence of $[Fe(CN)_6]^{3-/4-}$. However, after the electrochemical polymerization of 1,8-Diaminonaphthalene on the surface of the modified electrode, the current registered is around 82 µA which represent only 25.87% of initial current. This behavior is probably due the loss of conductivity of the polymer in neutral pH (Majid et al., 2003). It should be noted that a significant decrease in the value of ΔE_p was observed on poly 1,8-DAN/Cys/CB (blue line), which is equal to 83 mV. This could be attributed to the electrocatalytic behavior of poly 1,8-Diaminonaphthalene which enhances the electronic transfer. The same behavior was found by Oularbi et al., when using carbon nanofibers (CNF) combined with polypyrrole (PPy) (Oularbi et al., 2017).

In order to better understand the behavior at the interface electrode-solution of both electrodes unmodified and modified GCE, electrochemical impedance spectroscopy (EIS) was conducted at an applied potential of 350 mV *vs.* Ag/AgCl over a frequency range between 10 Hz and 100 KHz. The EIS is a well-known and powerful tool to investigate the electrochemical behaviors at the electrode–electrolyte interface (Ruiz-Camacho et al., 2017). Useful information can be extracted from the corresponding Nyquist plots such as the charge transfer resistance (R_{ct}) located at high frequencies, and the capacitance of the double layer located at low frequencies which is attributed to the diffusional process (Oularbi et al., 2020; Seenivasan et al., 2015). The corresponding Nyquist Plots with the equivalent circuit of poly 1,8-DAN/Cys/CB/GCE are presented in Fig. 3b. It can be seen that the semicircle of GCE (black line) is large with a charge transfer resistance (R_{ct}) of 52.55 Ω. While at the surface of poly 1,8 DAN /Cys/CB/

GCE (blue line), an important decrease of R_{ct} of about 0.0582 Ω was observed indicating a significant decrease of charge transfer resistance. These results suggest that the combination of thiol and amine groups with CB improves the electronic transfer ability of the electrodes. It should be noted that in the presence of CB and Cys/CB, the R_{ct} have been further decreased indicating an enhancement of the electronic transfer. In fact, CB improves the electronic transfer ability of the electrodes as reported by Malha et al., (Malha et al., 2016).

The active surface area of GCE, CB/GCE, and poly 1,8-DAN/Cys/CB/GCE have been calculated using Randles-Secvik equation described in the following equation noted (1) (Halim et al., 2019):

$$Ip = 2.69 \times 10^5 \times n^{\frac{3}{2}} \times A \times C \times D^{\frac{1}{2}} \times V^{\frac{1}{2}}$$

Where, the number of electrons transferred (n) is equal to 1, the concentration of $[Fe(CN)_6]^{3-/4-}$ (C) is equal to 10 mM and the diffusion coefficient (D) is equal to 6.7 10^{-6} cm^2/s. The effective surfaces were found to be 0.057 ± 0.001 cm^2, 0.118 ± 0.003 cm^2, and 0.023 ± 0.005 cm^2 for GCE, CB/GCE, and poly 1,8-DAN/CB/GCE respectively. In fact, the surface increased after the addition of carbon black as mentioned earlier by many authors (Deroco et al., 2018; Ibáñez-Redín et al., 2018). While, poly 1,8-DAN/Cys/CB/GCE had the smallest surface area. This behavior may be due the loss of conductivity of the poly 1,8-Diaminonaphthalene at neutral pH (Majid et al., 2003).

3.4. Electrochemical responses of the developed sensor toward nitrite ions

The applicability of the elaborated electrodes was then tested towards nitrite ions sensing. The determination of 1 mM of Nitrite was performed at pH 7.2 in phosphate buffer solution using cyclic voltammetry between 0 and 1.2 V *vs.* Ag/AgCl at 50 mV/s. The corresponding curves are shown in Fig. 4a. It is obvious that nitrite can be irreversibly oxidized on all the electrodes. At the surface of GCE (black line), a small and large peak was observed at the potential of 0.94 V *vs.* Ag/AgCl indicating that nitrite ions are hardly oxidized on the surface of GCE. After the modification of the electrode surface with CB suspension (red line), a decrease of about 100 mV was observed concerning the oxidation potential which was accompanied with a significant increase of the current intensity. This may be due to the large surface area of CB nanoparticles (Arduini et al., 2020). The electrodeposition of 1,8-Diaminonaphthalene on CB/GCE induced a well-defined peak (green line) at 0.82 V with an increase of the oxidation current. It should be mentioned that after the addition of Cysteine, the peak potential (blue line) decreased to more negative value (0.8 V *vs.* Ag/AgCl) with a further increase of the oxidation current showing the superior performance of poly 1,8-DAN/Cys/CB/GCE towards nitrite oxidation. This can be ascribed to the synergistic effect between amine groups of poly (1,8-diaminonaphthalene) and the thiol groups of cysteine. Indeed, Wang et al., and Gligor et al., have reported that an amine and thiol rich surfaces promotes the electrooxidation of nitrite (Wang et al., 2016; Gligor et al., 2017). Noting that an immobilization time of cysteine of 3 min offered the best results.

To determinate the nature of the electrode process, the effect of the scan rates on nitrite oxidation was investigated

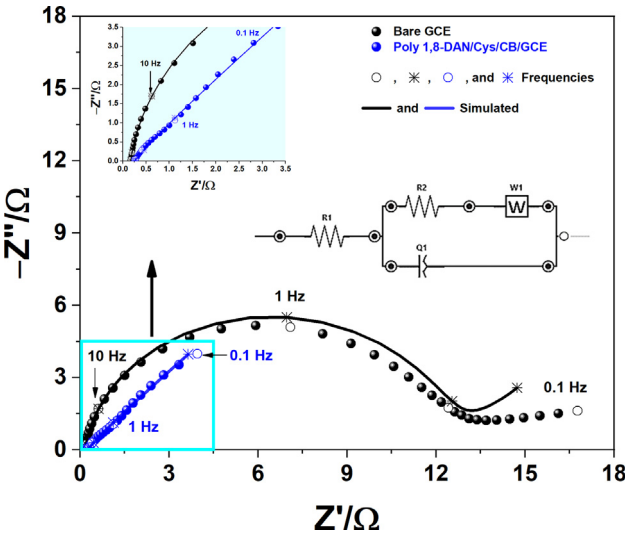

Fig. 5 Nyquist Plots of GCE (black line), and poly 1,8-DAN/Cys/CB/GCE (blue line) in pH 7.2, 0.1 M PBS containing 1 mM of NO_2^- at a fixed potential of 0.8 V *vs.* Ag/AgCl and an amplitude of 10 mV.

in the same solution (Fig. 4b). A linear regression was found between the anodic peak potential and the square root of scan rate according to the equation Ipa = −22.244263 + 249.93 83 $V^{\varnothing}$ (R^2 = 0.99417), confirming a diffusion-controlled process (Mehmeti et al., 2016). Same behavior was observed by Zhao et al., when using cobalt oxide combined with reduced graphene oxide and carbon nanotubes (Zhao et al., 2019). The plot of E_{pa} *vs.* Log V was found to be linear which confirms the irreversibility of the process (E_{pa} = 0.06928 Log V + 0.70011, R^2 = 0.9811). Based on these results, the number of the transferred electrons during the electrochemical oxidation of nitrite ions was calculated using the Laviron's Eq. (1) (Zhe et al., 2022; Suma et al., 2019):

$$E_{pa} = 2.3(RT/\alpha nF)LogV + K \quad (1)$$

Where, n is the number of the transferred electrons, α is the electron transfer coefficient taken as 0.5 in a totally irreversible reaction, R is the ideal gas constant (8.3145 J K^{-1} mol^{-1}), T is temperature (298.15 K), F is the Faraday constant (96485.33 A mol^{-1}), and V is the scan rate. The number of the transfer electrons was found to b 1.7 indicating that the electrochemical oxidation of nitrite ions involves the transfer of 2 electrons according the following mechanism (2) (Suma et al., 2019; Zou et al., 2017; He and Yan, 2019):

$$NO_2^- + H_2O \rightarrow NO_3^- + 2H^+ + 2\,e^- \quad (2)$$

In order to confirm the results obtained by CV experiments, EIS was performed in the same solution at the potential of 0.85 V *vs.* Ag/AgCl. The corresponding Nyquist plots are presented in Fig. 5. The difference between the unmodified GCE (black line) and Poly 1,8-Diaminonaphthalene/Cys/CB modified GCE (blue line) was significant and noticeable. Indeed, the semicircle part of the graph corresponding to the charge transfer resistance was reduced dramatically after the modification of the electrode (i.e., from 12000 Ω for bare electrode to 0.009 Ω for poly 1,8-DAN/Cys/CB/GCE. These results

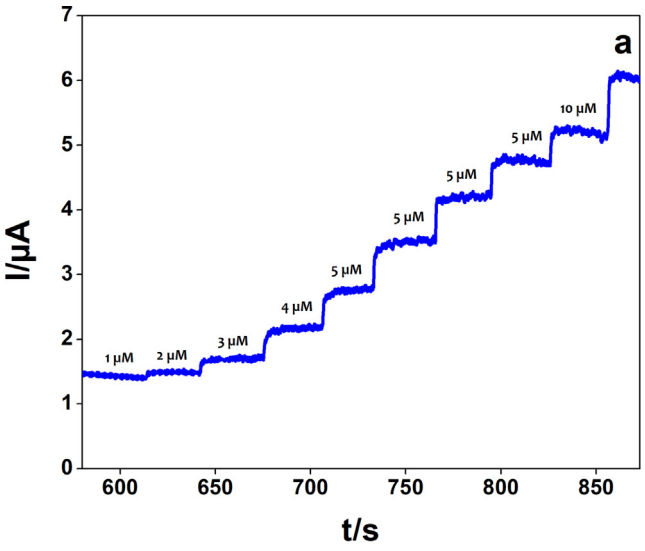

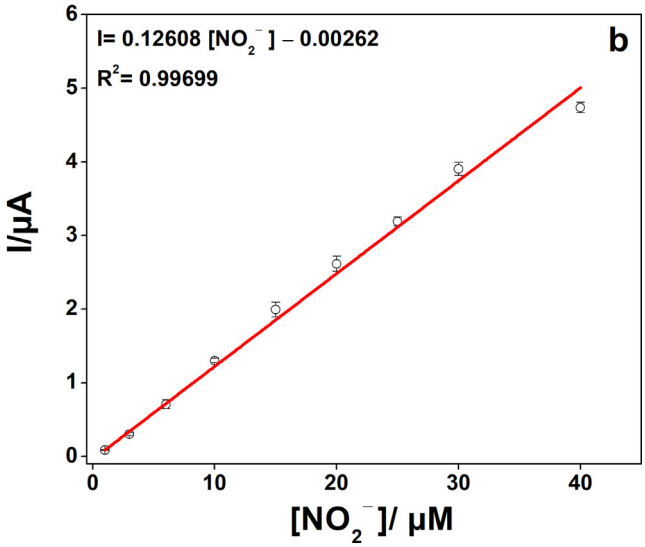

Fig. 6 **a)** Amperometry of poly 1,8-DAN/Cys/CB/GCE in pH 7.2, 0.2 M PBS, a fixed potential of 0.85 V *vs.* Ag/AgCl, and successive injections of NO_2^-. **b)** The calibration plot of the oxidation current versus NO_2^- concentration.

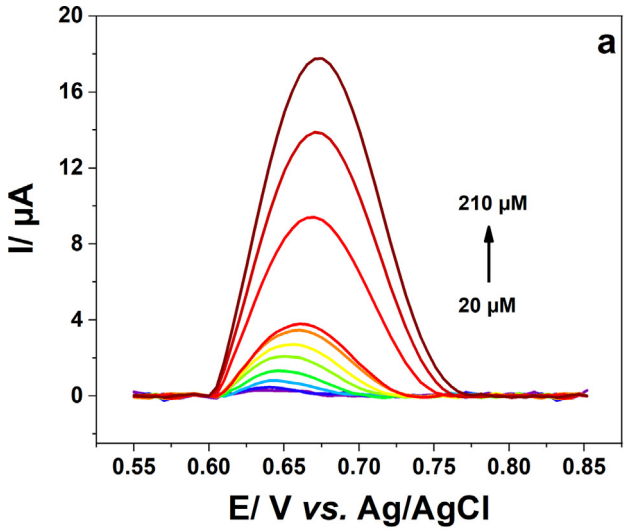

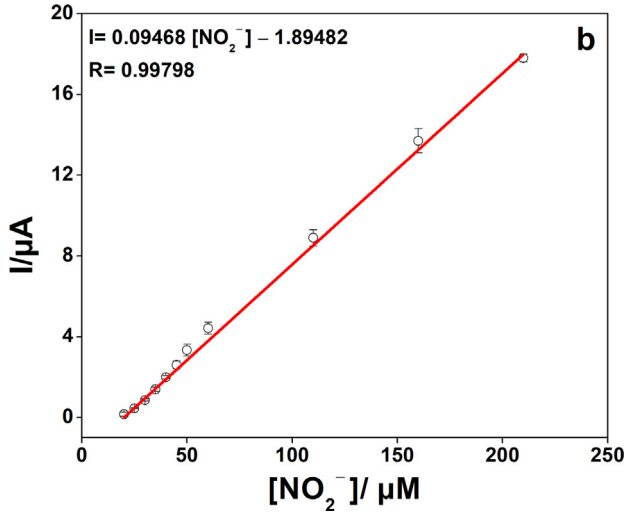

Fig. 7 **a)** Differential pulse voltammetry of poly 1,8-DAN/Cys/CB/GCE in pH 7.2, 0.2 M PBS, and a range of NO_2^- concentration from 20 to 210 µM. **b)** The calibration plot of the oxidation current versus NO_2^- concentration.

demonstrates the fast diffusion of nitrite ions into the surface of the catalyst (Oularbi et al., 2017; Islam et al., 2020). Based on the results observed using CV and EIS, we can assume that the modification of GCE induced a superior electrochemical behavior of the modified electrode towards target nitrite ions.

3.5. Electrochemical detection of nitrite

After the exploration of the electrochemical behavior of our catalyst, and in order to evaluate the analytical performances of poly 1,8-DAN/Cys/CB, the prepared composite was applied for the detection of nitrite ions using the amperometry and the differential pulse voltammetry (DPV) techniques. In the first experiment, the electrode was placed in a solution of 0.2 M PBS at pH 7.2. The subsequent injections of nitrite were performed under continuous stirring at a fixed potential of 0.85 V *vs.* Ag/AgCl (Fig. 6). Amperometry showed a linearity between the anodic current and the concentration range from 1 µM to 40 µM with an RSD of 2.07% (R^2 = 0.99699, 3 tests). The time response was about 2 s and the detection limit was determined to be 0.25 µM (S/N = 3).

We have also examined the response of the developed material by using another electrochemical technique which is differential pulse voltammetry. The measurements were conducted in 0.2 M PBS, from 0.6 V to 0.8 V *vs.* Ag/AgCl with an increment potential 0.005 V, Amplitude 0.1 V, and pulse width 0.05 s. The corresponding plots are displayed Fig. 7.

It can be seen that the intensity of the peaks is very closely related to the concentrations of nitrite. An excellent correlation coefficient (R^2 = 0.99798) was obtained for the concentrations of nitrite ranging from 20 µM to 210 µM with a relative standard deviation of 1.5% (3 tests). We can conclude that both techniques amperometry and DPV can detect nitrite ions in a wide range of concentrations. Therefore, we can

Table 1 Performance parameters of different materials reported in the literature.

Electrode	Method of detection	LOD (μM)	Linear range (μM)	Sensitivity (μA/μM)	Ref.
LIG/f-MWCNT-AuNPs	SWV	0.9	10–140	–	(Nasraoui et al., 2021)
AgNPs/MWCNTs/GCE	DPV	0.095	1–100	0.19	(Wan et al., 2017)
AuNPs/graphene/MCE	DPV	0.1	0.3–720	–	(Wang et al., 2017)
Fe_2O_3/rGO/GCE	DPV	0.015	0.05–780	0.204	(Radhakrishnan et al., 2014)
rGO/ZnO/GCE	Amperometry	1.36	20–250	0.2754	(Rashed et al., 2020)
rGO-Co_3O_4@Pt/GCE	Amperometry	1.73	10–650	0.026	(Shahid et al., 2015)
Poly(AM-co-HEA-co-NVc)/MWCNT/GE	Amperometry	0.003	0.01–25	-	(Zhao et al., 2019)
Poly 1,8-DAN/Cys /CB/GCE	Amperometry	0.25	1–40	0.12608	This work
	DPV		20–210	0.09468	

LIG: Laser-induced graphene
MWCNT: Multi walled carbon nanotubes
AgNPs: Silver nanoparticles
AuNPS: Gold nanoparticles
MCE: Mixed cellulose ester
ERGO: Electrochemically reduced graphene oxide
Cu-TDPAT: Copper metal–organic framework
rGO: Reduced graphene oxide
ZnO: Zinc oxide
Co_3O_4: Cobalt oxide
Pt: Platinum
GE: Gold electrode
AM: Acrylamide
HEA: 2-hydroxyethyl acrylate
NVc: N-vinyl carbazole

choose the most suitable technique depending on the required application. A quick comparison between the analytical performances of our material and some other materials reported in the literature is presented in Table 1. In fact, our material is low-priced compared to the other materials which are based on expensive metals such as gold, silver, and platinum (Chen et al., 2019; Shivakumar et al., 2017; Vijayaraj et al., 2017). Moreover, our approach allows a fast preparation of the sensor in less than 30 min, unlike the other approaches which are time consuming.

The stability and the reproducibility are important parameters in assessing the performance of the sensor. The stability of the sensor over one week was tested, and only a slight change was observed i.e., The sensors retained 94% of its initial current response which indicates that the response of poly 1,8-DAN/Cys/CB/GCE over nitrite oxidation was stable over seven days (Vinoth Kumar et al., 2017). The reproducibility was examined using a series of five independent electrodes. The measurements were obtained with a relative standard deviation of 5.5 % which indicates a good reproducibility of the sensor (Zhang, 2018).

The selectivity of the sensor was also examined in the presence of some common interfering products such as NaCl, $NaNO_3$, Na_2SO_4, and Na_2CO_3 at high concentrations (50-fold excess). The data obtained during this experiment are reported in Fig. 8 (3 tests). The effect of these interfering species on nitrite detection was not significant, which indicates the high selectivity of the sensors.

3.6. Real samples analysis

In order to verify the practical use of the proposed sensor, poly 1,8-DAN/Cys/CB/GCE was used for the determination of nitrite ions in water samples using amperometry. Fig. 9 illustrates a typical amperometry graph of successive additions of nitrite. To inquire more about the effective application of poly 1,8-DAN/Cys/CB/GCE for NO_2^- detection, the recovery evaluation was realized. The well water, tap water, and mineral water samples were spiked with different concentrations of NO_2^- (Table 2). The recoveries were found around 100% with an RSD below 4 % which indicates that the proposed sensor is suitable for application in these types of matrices.

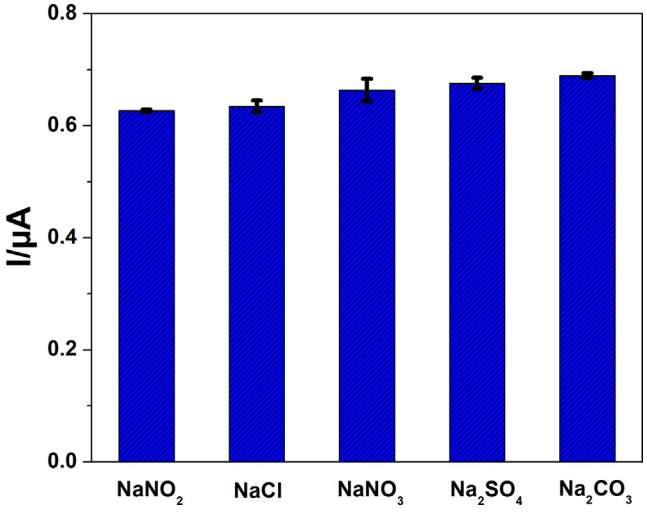

Fig. 8 Variation of NO_2^- oxidation current in the presence of some common interfering products.

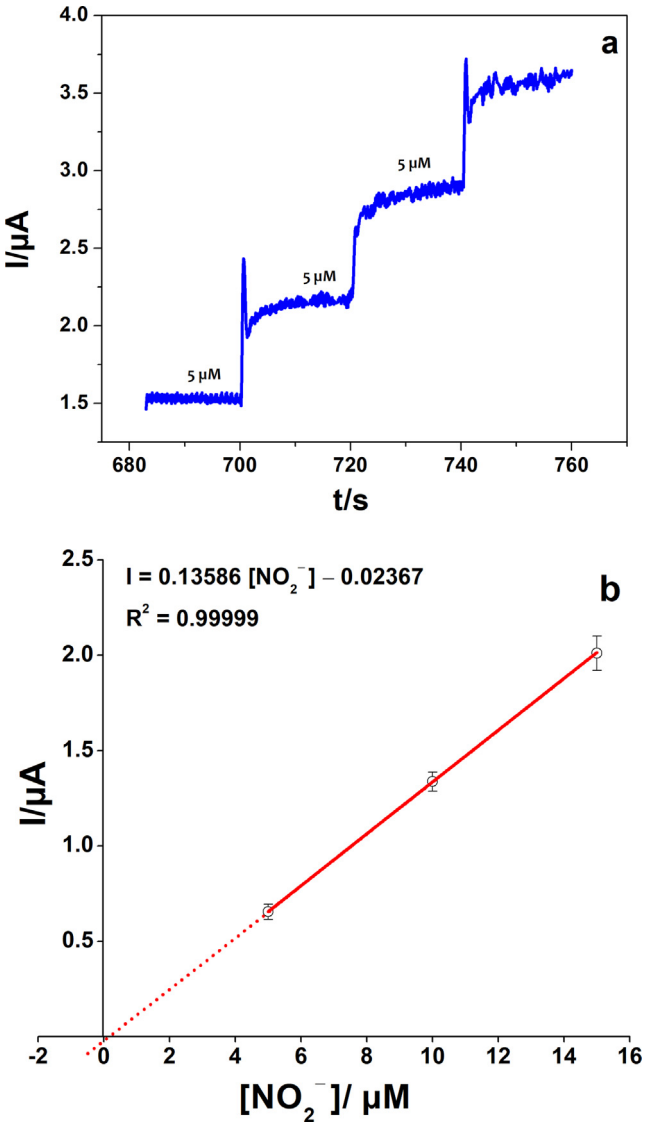

Fig. 9 **a)** Amperometry curve of NO_2^- detection in well water using poly 1,8-DAN/Cys/CB/GCE under the optimized experimental conditions. **b)** Linear corresponding curve for NO_2^- determination in tap water.

4. Conclusion

Poly (1,8-diaminonaphthalene) has been successfully synthesized onto cysteine/CB modified glassy carbon electrode using a quick and simple method in acidic medium. The prepared nanocomposites were carefully examined by using cyclic voltammetry and electrochemical impedance spectroscopy revealing an excellent electroactivity towards nitrite ions. An enhancement in the current intensity and a significant decrease in the charge transfer resistance were noted with a wide range of linearity and a low limit of detection. It seems that the combination of thiol and amine groups with carbon black induces a superior performance towards nitrite sensing, and displays an excellent reproducibility, stability, and also selectivity in the presence of some common interfering components. The sensor revealed a detection limit of 0.25 µM and two linearity ranges (R^2 above 0.99) from 1 µM to 40 µM and from 20 µM to 210 µM depending on the method used (amperometry or the differential pulse voltammetry). The sensor was then applied in different matrices and showed excellent recoveries around 100%, which demonstrates that our sensor is an outstanding choice for nitrite monitoring in real water samples.

Table 2 Recovery and relative standard deviation (RSD) of NO_2^- in the tap water samples using poly 1,8-DAN/Cys/CB/GCE (n = 3).

Sample	Added (µM)	Found (µM)	Recovery (%)	RSD (%)
Well water	**5**	5.17	103.4	1.8
	10	10.6	106	3.7
	15	15.8	105.3	1.6
Tap water	**5**	5.02	100.4	2.7
Mineral water containing Nitrates (5.18 µM)	**5**	5.11	102.2	2.3

Acknowledgement

This work was supported by MESRSFC (Ministère de l'Enseignement Supérieur et de la Recherche Scientifique et de la Formation des cadres - Morocco) and CNRST (Centre National pour la Recherche Scientifique et Technique-Morocco), (project number PPR/2015/72).

References

Annalakshmi, M., Balaji, R., Chen, S.-M., Chen, T.-W., Huang, Y., 2020. A sensitive and high-performance electrochemical detection of nitrite in water samples based on Sonochemical synthesized Strontium Ferrite Nanochain architectures. Electrochimica Acta. 360, 136797. https://doi.org/10.1016/j.electacta.2020.136797.

Buller, I.D., Patel, D.M., Weyer, P.J., Prizment, A., Jones, R.R., Ward, M.H., 2021. Ingestion of Nitrate and Nitrite and Risk of Stomach and Other Digestive System Cancers in the Iowa Women's Health Study. Int. J. Environ. Res. Public. Health. 18, 6822. https://doi.org/10.3390/ijerph18136822.

Mudan, A., Repplinger, D., Lebin, J., Lewis, J., Vohra, R., Smollin, C., 2020. Severe Methemoglobinemia and Death From Intentional Sodium Nitrite Ingestions. J. Emerg. Med. 59 (3), e85–e88. https://doi.org/10.1016/j.jemermed.2020.06.031.

Organization, W.H., 2011. Guidelines for drinking-water quality: World Health Organization. Distrib. Sales Geneva. 27.

Cvetković, D., Živković, V., Lukić, V., Nikolić, S., 2019. Sodium nitrite food poisoning in one family. Forensic Sci. Med. Pathol. 15 (1), 102–105. https://doi.org/10.1007/s12024-018-0036-1.

Wu, S., Thapa, B., Rivera, C., Yuan, Y., 2021. Nitrate and nitrite fertilizer production from air and water by continuous flow liquid-phase plasma discharge. J. Environ. Chem. Eng. 9 (2), 104761.

Wang, Q.-H., Yu, L.-J., Liu, Y., Lin, L., Lu, R.-G., Zhu, J.-P., et al, 2017. Methods for the detection and determination of nitrite and nitrate: A review. Talanta. 165, 709–720. https://doi.org/10.1016/j.talanta.2016.12.044.

Mahmud, M.A.P., Ejeian, F., Azadi, S., Myers, M., Pejcic, B., Abbassi, R., et al, 2020. Recent progress in sensing nitrate, nitrite, phosphate, and ammonium in aquatic environment. Chemosphere. 259, 127492. https://doi.org/10.1016/j.chemosphere.2020.127492.

Mako, T.L., Levenson, A.M., Levine, M., 2020. Ultrasensitive Detection of Nitrite through Implementation of *N* -(1-Naphthyl) ethylenediamine-Grafted Cellulose into a Paper-Based Device. ACS Sens. 5 (4), 1207–1215. https://doi.org/10.1021/acssensors.0c00291.

Zanfrognini, B., Pigani, L., Zanardi, C., 2020. Recent advances in the direct electrochemical detection of drugs of abuse. J. Solid State

Electrochem. 24 (11-12), 2603–2616. https://doi.org/10.1007/s10008-020-04686-z.

El Rhazi, M., Majid, S., Elbasri, M., Salih, F.E., Oularbi, L., Lafdi, K., 2018. Recent progress in nanocomposites based on conducting polymer: application as electrochemical sensors. Int. Nano Lett. 8 (2), 79–99. https://doi.org/10.1007/s40089-018-0238-2.

Oularbi, L., Turmine, M., Salih, F.E., El Rhazi, M., 2020. Ionic liquid/carbon nanofibers/bismuth particles novel hybrid nanocomposite for voltammetric sensing of heavy metals. J. Environ. Chem. Eng. 8 (3), 103774.

Oularbi, L., Turmine, M., El Rhazi, M., 2019. Preparation of novel nanocomposite consisting of bismuth particles, polypyrrole and multi-walled carbon nanotubes for simultaneous voltammetric determination of cadmium(II) and lead(II). Synth. Met. 253, 1–8. https://doi.org/10.1016/j.synthmet.2019.04.011.

Salih, F.E., Ouarzane, A., El Rhazi, M., 2017. Electrochemical detection of lead (II) at bismuth/Poly(1,8-diaminonaphthalene) modified carbon paste electrode. Arab. J. Chem. 10 (5), 596–603. https://doi.org/10.1016/j.arabjc.2015.08.021.

Oularbi, L., 2018. Étude de nanocomposites polypyrrole/nanoparticule de carbone par impédance électrochimique et ac-électrogravimétrie: application aux capteurs électrochimiques, Sorbonne Université; Université Hassan II. Casablanca, Maroc.

Deroco, P.B., Rocha-Filho, R.C., Fatibello-Filho, O., 2018. A new and simple method for the simultaneous determination of amoxicillin and nimesulide using carbon black within a dihexadecylphosphate film as electrochemical sensor. Talanta 179, 115–123. https://doi.org/10.1016/j.talanta.2017.10.048.

Deroco, P.B., Melo, I.G., Silva, L.S.R., Eguiluz, K.I.B., Salazar-Banda, G.R., Fatibello-Filho, O., 2018. Carbon black supported Au–Pd core-shell nanoparticles within a dihexadecylphosphate film for the development of hydrazine electrochemical sensor. Sens. Actuators B Chem. 256, 535–542. https://doi.org/10.1016/j.snb.2017.10.107.

Mazzaracchio, V., Tomei, M.R., Cacciotti, I., Chiodoni, A., Novara, C., Castellino, M., et al, 2019. Inside the different types of carbon black as nanomodifiers for screen-printed electrodes. Electrochimica Acta. 317, 673–683. https://doi.org/10.1016/j.electacta.2019.05.117.

Baccarin, M., Santos, F.A., Vicentini, F.C., Zucolotto, V., Janegitz, B. C., Fatibello-Filho, O., 2017. Electrochemical sensor based on reduced graphene oxide/carbon black/chitosan composite for the simultaneous determination of dopamine and paracetamol concentrations in urine samples. J. Electroanal. Chem. 799, 436–443. https://doi.org/10.1016/j.jelechem.2017.06.052.

Ibáñez-Redín, G., Wilson, D., Gonçalves, D., Oliveira, O.N., 2018. Low-cost screen-printed electrodes based on electrochemically reduced graphene oxide-carbon black nanocomposites for dopamine, epinephrine and paracetamol detection. J. Colloid Interface Sci. 515, 101–108. https://doi.org/10.1016/j.jcis.2017.12.085.

Bhatt, R., Mishra, A., Bajpai, A.K., 2021. Role of diaminonaphthalene based polymers as sensors in detection of biomolecules: A review. Results Mater. 9, 100174. https://doi.org/10.1016/j.rinma.2021.100174.

Chemchoub, S., Oularbi, L., El Attar, A., Younssi, S.A., Bentiss, F., Jama, C., et al, 2020. Cost-effective non-noble metal supported on conducting polymer composite such as nickel nanoparticles/polypyrrole as efficient anode electrocatalyst for ethanol oxidation. Mater. Chem. Phys. 250, 123009. https://doi.org/10.1016/j.matchemphys.2020.123009.

Halim, E.M., Perrot, H., Sel, O., Debiemme-Chouvy, C., Lafdi, K., El Rhazi, M., 2021. Electrosynthesis of hierarchical Cu_2O–$Cu(OH)_2$ nanodendrites supported on carbon nanofibers/poly(para-phenylenediamine) nanocomposite as high-efficiency catalysts for methanol electrooxidation. Int. J. Hydrog. Energy. 46 (38), 19926–19938. https://doi.org/10.1016/j.ijhydene.2021.03.119.

Shi, S., Li, Z., Chen, Y., Yang, J., Xu, H., Huang, J., et al, 2019. Electrochemically co-deposition of palladium nanoparticles and poly (1, 5-diaminonaphthalene) onto multiwalled carbon nanotubes (MWCNTs) modified electrode and its application for amperometric determination of nitrite. Int. J. Electrochem. Sci. 14, 7983–7994.

Chemchoub, S., Elbasri, M., Halim, E.M., El Rhazi, M., 2019. The electrocatalytic oxidation of methanol on a carbon paste electrode modified by poly (para-phenylenediamine) and Nickel particles. Mater. Today Proc. 13, 720–729.

Xiao, Q.i., Feng, M., Liu, Y.i., Lu, S., He, Y., Huang, S., 2018. The graphene/polypyrrole/chitosan-modified glassy carbon electrode for electrochemical nitrite detection. Ionics 24 (3), 845–859. https://doi.org/10.1007/s11581-017-2247-y.

Chen, G., Zheng, J., 2021. Non-enzymatic electrochemical sensor for nitrite based on a graphene oxide–polyaniline–Au nanoparticles nanocomposite. Microchem. J. 164, 106034. https://doi.org/10.1016/j.microc.2021.106034.

Ge, Y.i., Jamal, R., Zhang, R., Zhang, W., Yu, Z., Yan, Y., et al, 2020. Electrochemical synthesis of multilayered PEDOT/PEDOT-SH/Au nanocomposites for electrochemical sensing of nitrite. Microchim. Acta. 187 (4). https://doi.org/10.1007/s00604-020-4211-1.

Salhi, O., Ez-zine, T., El Rhazi, M., 2021. Hybrid Materials Based on Conducting Polymers for Nitrite Sensing: A Mini Review. Electroanalysis 33 (7), 1681–1690. https://doi.org/10.1002/elan.202100033.

El Attar, A., Chemchoub, S., Diallo Kalan, M., Oularbi, L., El Rhazi, M., 2022. Designing New Material Based on Functionalized Multi-Walled Carbon Nanotubes and $Cu(OH)_2$–Cu_2O/Polypyrrole Catalyst for Ethanol Oxidation in Alkaline Medium. Front. Chem. 9. https://doi.org/10.3389/fchem.2021.805654.

El Attar, A., Oularbi, L., Chemchoub, S., El Rhazi, M., 2020. Preparation and characterization of copper oxide particles/polypyrrole (Cu2O/PPy) via electrochemical method: Application in direct ethanol fuel cell. Int. J. Hydrog. Energy. 45 (15), 8887–8898. https://doi.org/10.1016/j.ijhydene.2020.01.008.

El Attar, A., Oularbi, L., Chemchoub, S., El Rhazi, M., 2021. Effect of electrochemical activation on the performance and stability of hybrid (PPy/Cu2O nanodendrites) for efficient ethanol oxidation in alkaline medium. J. Electroanal. Chem. 885, 115042. https://doi.org/10.1016/j.jelechem.2021.115042.

Kaladevi, G., Wilson, P., Pandian, K., 2020. Simultaneous and Selective Electrochemical Detection of Sulfite and Nitrite in Water Sources Using Homogeneously Dispersed Ag Nanoparticles over PANI/rGO Nanocomposite. J. Electrochem. Soc. 167 (2), 027514. https://doi.org/10.1149/1945-7111/ab6973.

Ma, X., Miao, T., Zhu, W., Gao, X., Wang, C., Zhao, C., et al, 2014. Electrochemical detection of nitrite based on glassy carbon electrode modified with gold–polyaniline–graphene nanocomposites. RSC Adv. 4 (101), 57842–57849. https://doi.org/10.1039/C4RA08543D.

Majid, S., Rhazi, M.E., Amine, A., Curulli, A., Palleschi, G., 2003. Carbon Paste Electrode Bulk-Modified with the Conducting Polymer Poly(1,8-Diaminonaphthalene): Application to Lead Determination. Microchim. Acta. 143 (2-3), 195–204. https://doi.org/10.1007/s00604-003-0058-5.

Hwa, K.-Y., Sharma, T.S.K., Karuppaiah, P., 2019. Development of an electrochemical sensor based on a functionalized carbon black/tungsten carbide hybrid composite for the detection of furazolidone. New J. Chem. 43 (30), 12078–12086. https://doi.org/10.1039/C9NJ02531F.

Oyama, N., Sato, M., Ohsaka, T., 1989. Preparation of thin polymeric films on electrode surfaces by electro-polymerization of aromatic compounds with amino groups. Synth. Met. 29 (1), 501–506. https://doi.org/10.1016/0379-6779(89)90340-8.

Tagowska, M., Pałys, B., Mazur, M., Skompska, M., Jackowska, K., 2005. In situ deposition of poly(1,8-diaminonaphthalene): from thin films to nanometer-sized structures. Electrochimica Acta. 50 (12), 2363–2370. https://doi.org/10.1016/j.electacta.2004.10.049.

Sanders, W., Anderson, M.R., 2009. Electrostatic deposition of polycations and polyanions onto cysteine monolayers. J. Colloid Interface Sci. 331 (2), 318–321. https://doi.org/10.1016/j.jcis.2008.12.010.

Nguyen, D.T., Tran, L.D., Le Nguyen, H., Nguyen, B.H., Van Hieu, N., 2011. Modified interdigitated arrays by novel poly(1,8-diaminonaphthalene)/carbon nanotubes composite for selective detection of mercury(II). Talanta 85 (5), 2445–2450. https://doi.org/10.1016/j.talanta.2011.07.094.

Lee, J.-W., Park, D.-S., Shim, Y.-B., Park, S.-M., 1992. Electrochemical Characterization of Poly(1,8-diaminonaphthalene): A Functionalized Polymer. J. Electrochem. Soc. 139 (12), 3507–3514. https://doi.org/10.1149/1.2069107.

Cinti, S., Arduini, F., Carbone, M., Sansone, L., Cacciotti, I., Moscone, D., et al, 2015. Screen-Printed Electrodes Modified with Carbon Nanomaterials: A Comparison among Carbon Black, Carbon Nanotubes and Graphene. Electroanalysis 27 (9), 2230–2238. https://doi.org/10.1002/elan.201500168.

Kingsford, O.J., Zhang, D., Ma, Y., Wu, Y., Zhu, G., 2019. Electrochemically Recognizing Tryptophan Enantiomers based on Carbon Black/Poly-l-Cysteine Modified Electrode. J. Electrochem. Soc. 166 (13), B1226–B1231. https://doi.org/10.1149/2.0791913jes.

He, D., Peng, Z., Gong, W., Luo, Y., Zhao, P., Kong, L., 2015. Mechanism of a green graphene oxide reduction with reusable potassium carbonate. RSC Adv. 5 (16), 11966–11972. https://doi.org/10.1039/C4RA14511A.

Xie, Y., Zhang, S.-H., Jiang, H.-Y., Zeng, H., Wu, R.-M., Chen, H., et al, 2019. Properties of carbon black-PEDOT composite prepared via in-situ chemical oxidative polymerization. E-Polym. 19 (1), 61–69. https://doi.org/10.1515/epoly-2019-0008.

Dokken, K.M., Parsons, J.G., McClure, J., Gardea-Torresdey, J.L., 2009. Synthesis and structural analysis of copper(II) cysteine complexes. Inorganica Chim. Acta. 362 (2), 395–401. https://doi.org/10.1016/j.ica.2008.04.037.

Parsons, J.G., Dokken, K.M., McClure, J., Gardea-Torresdey, J.L., 2013. FTIR, XAS, and XRD study of cadmium complexes with l-cysteine. Polyhedron 56, 237–242. https://doi.org/10.1016/j.poly.2013.04.001.

Nasalska, A., Skompska, M., 2003. Removal of toxic chromate ions by the films of poly(1,8-diaminonaphthalene). J. Appl. Electrochem. 33, 113–119. https://doi.org/10.1023/A:1022952019530.

Pałys, B.J., Skompska, M., Jackowska, K., 1997. Sensitivity of poly 1,8-diaminonaphthalene to heavy metal ions — electrochemical and vibrational spectra studies. J. Electroanal. Chem. 433 (1-2), 41–48. https://doi.org/10.1016/S0022-0728(97)00144-7.

Arduini, F., Cinti, S., Mazzaracchio, V., Scognamiglio, V., Amine, A., Moscone, D., 2020. Carbon black as an outstanding and affordable nanomaterial for electrochemical (bio)sensor design. Biosens. Bioelectron. 156, 112033. https://doi.org/10.1016/j.bios.2020.112033.

Oularbi, L., Turmine, M., El Rhazi, M., 2017. Electrochemical determination of traces lead ions using a new nanocomposite of polypyrrole/carbon nanofibers. J. Solid State Electrochem. 21 (11), 3289–3300. https://doi.org/10.1007/s10008-017-3676-2.

Ruiz-Camacho, B., Baltazar Vera, J.C., Medina-Ramírez, A., Fuentes-Ramírez, R., Carreño-Aguilera, G., 2017. EIS analysis of oxygen reduction reaction of Pt supported on different substrates. Int. J. Hydrog. Energy. 42 (51), 30364–30373. https://doi.org/10.1016/j.ijhydene.2017.08.087.

Seenivasan, R., Chang, W.-J., Gunasekaran, S., 2015. Highly Sensitive Detection and Removal of Lead Ions in Water Using Cysteine-Functionalized Graphene Oxide/Polypyrrole Nanocomposite Film Electrode. ACS Appl. Mater. Interfaces. 7 (29), 15935–15943. https://doi.org/10.1021/acsami.5b03904.

Malha, S.I.R., Lahcen, A.A., Arduini, F., Ourari, A., Amine, A., 2016. Electrochemical Characterization of Carbon Solid-like Paste Electrode Assembled Using Different Carbon Nanoparticles. Electroanalysis. 28 (5), 1044–1051. https://doi.org/10.1002/elan.201500637.

Halim, E.M., Elbasri, M., Perrot, H., Sel, O., Lafdi, K., El Rhazi, M., 2019. Synthesis of carbon nanofibers/poly(para-phenylenediamine)/nickel particles nanocomposite for enhanced methanol electrooxidation. Int. J. Hydrog. Energy. 44 (45), 24534–24545. https://doi.org/10.1016/j.ijhydene.2019.07.141.

Wang, X., Cao, T., Zuo, Q., Wu, S., Uchiyama, S., Matsuura, H., 2016. Sensitive nitrite detection using a simple electrochemically aminated glassy carbon electrode. Anal. Methods 8 (17), 3445–3449. https://doi.org/10.1039/C6AY00015K.

Gligor, D., Cuibus, F., Peipmann, R., Bund, A., 2017. Novel amperometric sensors for nitrite detection using electrodes modified with PEDOT prepared in ionic liquids. J. Solid State Electrochem. 21 (1), 281–290. https://doi.org/10.1007/s10008-016-3368-3.

Mehmeti, E., Stanković, D.M., Hajrizi, A., Kalcher, K., 2016. The use of graphene nanoribbons as efficient electrochemical sensing material for nitrite determination. Talanta 159, 34–39. https://doi.org/10.1016/j.talanta.2016.05.079.

Zhao, Z., Zhang, J., Wang, W., Sun, Y., Li, P., Hu, J., et al, 2019. Synthesis and electrochemical properties of Co_3O_4-rGO/CNTs composites towards highly sensitive nitrite detection. Appl. Surf. Sci. 485, 274–282. https://doi.org/10.1016/j.apsusc.2019.04.202.

Zhe, T., Li, M., Li, F., Li, R., Bai, F., Bu, T., et al, 2022. Integrating electrochemical sensor based on MoO_3/Co_3O_4 heterostructure for highly sensitive sensing of nitrite in sausages and water. Food Chem. 367, 130666. https://doi.org/10.1016/j.foodchem.2021.130666.

Suma, B.P., Adarakatti, P.S., Kempahanumakkagari, S.K., Malingappa, P., 2019. A new polyoxometalate/rGO/Pani composite modified electrode for electrochemical sensing of nitrite and its application to food and environmental samples. Mater. Chem. Phys. 229, 269–278. https://doi.org/10.1016/j.matchemphys.2019.02.087.

Zou, C., Yang, B., Bin, D., Wang, J., Li, S., Yang, P., et al, 2017. Electrochemical synthesis of gold nanoparticles decorated flower-like graphene for high sensitivity detection of nitrite. J. Colloid Interface Sci. 488, 135–141. https://doi.org/10.1016/j.jcis.2016.10.088.

He, B., Yan, D., 2019. Au/ERGO nanoparticles supported on Cu-based metal-organic framework as a novel sensor for sensitive determination of nitrite. Food Control. 103, 70–77. https://doi.org/10.1016/j.foodcont.2019.04.001.

Islam, T., Hasan, M.M., Akter, S.S., Alharthi, N.H., Karim, M.R., Aziz, M.A., et al, 2020. Fabrication of Ni–Co-Based Heterometallo-Supramolecular Polymer Films and the Study of Electron Transfer Kinetics for the Nonenzymatic Electrochemical Detection of Nitrite. ACS Appl. Polym. Mater. 2 (2), 273–284. https://doi.org/10.1021/acsapm.9b00797.

Chen, H., Yang, T., Liu, F., Li, W., 2019. Electrodeposition of gold nanoparticles on Cu-based metal-organic framework for the electrochemical detection of nitrite. Sens. Actuators B Chem. 286, 401–407. https://doi.org/10.1016/j.snb.2018.10.036.

Shivakumar, M., Nagashree, K.L., Manjappa, S., Dharmaprakash, M. S., 2017. Electrochemical Detection of Nitrite Using Glassy Carbon Electrode Modified with Silver Nanospheres (AgNS) Obtained by Green Synthesis Using Pre-hydrolysed Liquor. Electroanalysis 29 (5), 1434–1442. https://doi.org/10.1002/elan.201600775.

Vijayaraj, K., Jin, S.-H., Park, D.-S., 2017. A Sensitive and Selective Nitrite Detection in Water Using Graphene/Platinum Nanocomposite. Electroanalysis 29 (2), 345–351. https://doi.org/10.1002/elan.201600133.

Vinoth Kumar, J., Karthik, R., Chen, S.-M., Balasubramanian, P., Muthuraj, V., Selvam, V., 2017. A Novel Cerium Tungstate Nanosheets Modified Electrode for the Effective Electrochemical

Detection of Carcinogenic Nitrite Ions. Electroanalysis 29 (10), 2385–2394. https://doi.org/10.1002/elan.201700120.

Zhang, Y.u., 2018. Copper/hexagonal Boron Nitride Nanosheet Composite as an Electrochemical Sensor for Nitrite Determination. Int. J. Electrochem. Sci., 5995–6004 https://doi.org/10.20964/2018.06.23.

Nasraoui, S., Al-Hamry, A., Teixeira, P.R., Ameur, S., Paterno, L.G., Ben Ali, M., et al, 2021. Electrochemical sensor for nitrite detection in water samples using flexible laser-induced graphene electrodes functionalized by CNT decorated by Au nanoparticles. J. Electroanal. Chem. 880, 114893. https://doi.org/10.1016/j.jelechem.2020.114893.

Wan, Y., Zheng, Y.F., Wan, H.T., Yin, H.Y., Song, X.C., 2017. A novel electrochemical sensor based on Ag nanoparticles decorated multi-walled carbon nanotubes for applied determination of nitrite. Food Control 73, 1507–1513. https://doi.org/10.1016/j.foodcont.2016.11.014.

Wang, P., Wang, M., Zhou, F., Yang, G., Qu, L., Miao, X., 2017. Development of a paper-based, inexpensive, and disposable electrochemical sensing platform for nitrite detection. Electrochem. Commun. 81, 74–78. https://doi.org/10.1016/j.elecom.2017.06.006.

Radhakrishnan, S., Krishnamoorthy, K., Sekar, C., Wilson, J., Kim, S.J., 2014. A highly sensitive electrochemical sensor for nitrite detection based on Fe_2O_3 nanoparticles decorated reduced graphene oxide nanosheets. Appl. Catal. B Environ. 148–149, 22–28. https://doi.org/10.1016/j.apcatb.2013.10.044.

Rashed, M.A., Faisal, M., Harraz, F.A., Jalalah, M., Alsaiari, M., Al-Assiri, M.S., 2020. rGO/ZnO/Nafion nanocomposite as highly sensitive and selective amperometric sensor for detecting nitrite ions (NO2−). J. Taiwan Inst. Chem. Eng. 112, 345–356. https://doi.org/10.1016/j.jtice.2020.05.015.

Shahid, M.M., Rameshkumar, P., Pandikumar, A., Lim, H.N., Ng, Y.H., Huang, N.M., 2015. An electrochemical sensing platform based on a reduced graphene oxide–cobalt oxide nanocube@platinum nanocomposite for nitric oxide detection. J. Mater. Chem. A. 3 (27), 14458–14468. https://doi.org/10.1039/C5TA02608C.

Zhao, W., Yang, H., Xu, S., Li, X., Wei, W., Liu, X., 2019. "Olive-Structured" Nanocomposite Based on Multiwalled Carbon Nanotubes Decorated with an Electroactive Copolymer for Environmental Nitrite Detection. ACS Sustain. Chem. Eng. 7 (20), 17424–17431. https://doi.org/10.1021/acssuschemeng.9b04616.